

Improving coherence with nested environments

H. J. Moreno,^{1,2} T. Gorin,³ and T. H. Seligman^{2,4}

¹*Facultad de Ciencias, Universidad Autónoma del Estado de Morelos, Cuernavaca, Morelos, México.*

²*Instituto de Ciencias Físicas, Universidad Nacional Autónoma de México, Cuernavaca, México.*

³*Departamento de Física, Universidad de Guadalajara, Guadalajara, Jalisco, México.*

⁴*Centro Internacional de Ciencias A.C., Cuernavaca, México.*

For many experimental quantum information devices, the central system is well isolated against simple decoherence processes such as spontaneous emission or coupling to a heat bath, but it is subject to some imperfections in the apparatus. To describe this situation, we insert a near environment which provides the residual coupling between central system and heat bath, and neglect any direct couplings. In the framework of random matrix theory we calculate the decoherence of the central system, using a linear response expansion for the coupling to the far environment and a dephasing coupling between central system and near environment. We find that the increase of the coupling to the far environment will slow down the decoherence in the central system, and thus improve the quality of the device. We extend this result to stronger couplings by numerical calculations in a modified Caldeira-Leggett model.

PACS numbers: 03.65.Yz, 05.45.Mt, 42.50.Lc

Keywords: open quantum systems, random matrix theory, decoherence

In many quantum optics experiments and quantum information devices we find the following situation: The central system, well protected from simple decoherence processes such as spontaneous emission or direct coupling to a structureless heat bath, still suffers some decoherence from the coupling to or instabilities of the quantum part of the apparatus. We will call the former the far environment and the latter the near environment. An example results from the celebrated Haroche experiment [1, 2], if we interpret the two-level atom as the central system, the cavity as the near environment and its leaks and absorption as coupling to a far environment. In such situations, different strategies have been developed in order to deal with the residual decoherence process, such as using particular spectral density functions, describing a structured heat bath, non-Markovian quantum master equations [3], or incorporating some degrees of freedom of the environment into the central system Ref. [4].

Assuming a tripartite system without direct coupling between central system and far environment, we find that increasing the coupling of the near to the far environment can protect the central system against decoherence. This fact seems somewhat anti-intuitive but in the setting of the Haroche experiment the late M. C. Nemes discussed this possibility with one of the authors [5] twelve years ago. More recently, additional numerical evidence in various settings has appeared [6], some of which were master thesis related to the present work [7–9]. Finally, it was shown in a different setting that in a strong coupling limit a protected subspace can appear [10].

To obtain results with some claim of universality we use random matrix theory (RMT) of decoherence [11–13]. We simplify the picture by limiting the coupling between central system and near environment to dephasing, and assume the coupling between near and far environment to

be separable. In this setup, many analytical expressions exist [14–18] in the absence of the far environment, we can take the advantage of these expressions, if we treat the far environment within a linear response calculation. We thus obtain analytic expressions for weak couplings between near and far environment. To study the effect of the far environment beyond the linear response approximation, we perform numerical simulations, using a modified Caldeira-Leggett master equation [19], whose equivalence to RMT models has first been discussed in Ref. [20].

Model: The full system consists of three parts, the central system, the near environment and the far environment with Hilbert spaces \mathcal{H}_c , \mathcal{H}_e and \mathcal{H}_f . The unitary evolution of the entire system is given by the Hamiltonian

$$H_{\text{tot}} = H_0 + v_c \otimes V_e \otimes \mathbb{1}_f + \gamma \mathbb{1}_c \otimes V'_e \otimes V_f \quad (1)$$

where $H_0 = h_c \otimes \mathbb{1}_{e,f} + \mathbb{1}_c \otimes H_e \otimes \mathbb{1}_f + \mathbb{1}_{c,e} \otimes H_f$. Tracing out both environments leads to the reduced dynamics of the central system $\varrho_c(t) = \text{tr}_{e,f}[\varrho_{\text{tot}}(t)]$, with

$$\varrho_{\text{tot}}(t) = \exp(-iH_{\text{tot}}t/\hbar) \varrho_c \otimes \varrho_{e,f} \exp(iH_{\text{tot}}t/\hbar), \quad (2)$$

where ϱ_c represents the initial state of the central system (typically assumed to be pure), and $\varrho_{e,f}$ represents the initial states of the environment. The separable couplings are given by $v_c \otimes V_e$ (between central system and near environment) and $\gamma V'_e \otimes V_f$ (between near and far environment). The former will be chosen as dephasing, such that $[h_c, v_c] = 0$. Such couplings are frequently used for open systems [3], as they simplify calculations and maintain many essential properties.

Dynamics: We write the Hamiltonian as $H_{\text{tot}} = \sum_j |j\rangle\langle j| \otimes H_{e,f}^{(j)}$, with

$$H_{e,f}^{(j)} = (\varepsilon_j \mathbb{1}_e + H_e + \nu_j V_e) \otimes \mathbb{1}_f + \mathbb{1}_e \otimes H_f + \gamma V'_e \otimes V_f, \quad (3)$$

where the set of states $\{|j\rangle\}_j$ is a common eigenbasis of h_c and v_c , while ε_j and ν_j are the corresponding eigenvalues. The evolution of the whole system can be written as $\varrho_{\text{tot}}(t) = \sum_{jk} \rho_{jk}(0) |j\rangle\langle k| \otimes \varrho^{(j,k)}(t)$, where $\varrho_c = \sum_{jk} \rho_{jk}(0) |j\rangle\langle k|$ is the initial state of the central system, and

$$\varrho^{(j,k)}(t) = \exp(-iH_{e,f}^{(j)}t/\hbar) \varrho_{e,f} \exp(iH_{e,f}^{(k)}t/\hbar). \quad (4)$$

We find for the matrix elements of the reduced state of the central system: $\rho_{jk}(t) = \rho_{jk}(0) \text{tr}_{e,f}[\varrho^{(j,k)}(t)]$. Since $\text{tr}_{e,f}[\varrho^{(j,j)}(t)] = 1$, the diagonal elements are constant in time, while the off-diagonal ones (i.e. the coherences) are given as expectation values of generalized echo operators in the composite environment.

In other words focussing on an individual matrix element, $\rho_{jk}(t)$, we may introduce

$$H_\lambda = H_0 + \lambda V_{\text{eff}} = H_e + \nu_j V_e, \quad H_0 = H_e + \nu_k V_e, \quad (5)$$

such that $\lambda V_{\text{eff}} = (\nu_j - \nu_k) V_e$. This allows to connect the coherences for vanishing coupling ($\gamma \rightarrow 0$) to the far environment, with fidelity amplitudes [14, 15]. Introducing the relative coherences

$$f_{\lambda,\gamma}(t) = \frac{\rho_{jk}(t)}{\rho_{jk}(0)} = \text{tr}_{e,f}[e^{-iH_{\lambda,\gamma}t/\hbar} \varrho_{e,f} e^{iH_{0,\gamma}t/\hbar}], \quad (6)$$

where $H_{\lambda,\gamma} = H_\lambda \otimes \mathbb{1}_f + \mathbb{1}_e \otimes H_f + \gamma V_e' \otimes V_f$, we find that $f_{\lambda,0}(t) \equiv f_\lambda(t)$ with

$$f_\lambda(t) = \text{tr}_e[M_\lambda(t) \text{tr}_f(\varrho_{e,f})], \quad M_\lambda(t) = e^{iH_0t/\hbar} e^{-iH_\lambda t/\hbar}. \quad (7)$$

Hence, $f_{\lambda,0}(t)$ becomes the fidelity amplitude for perturbing the Hamiltonian H_0 by λV_{eff} , given the initial state $\text{tr}_f(\varrho_{e,f})$ in the near environment.

Perturbative calculation: Applying the linear response approximation in the Fermi golden rule regime to the coupling between near and far environment, one arrives after some lengthy but straight forward algebra [21] at

$$f_{\lambda,\Gamma}(t) \sim (1 - \Gamma t) f_\lambda(t) + \Gamma \int_0^t d\tau f_\lambda(\tau) f_\lambda(t - \tau), \quad (8)$$

with the transition rate $\Gamma = \gamma^2 \tau_H N_e / \hbar^2$ (τ_H is the Heisenberg time in the far environment, and N_e is the dimension of the near environment). Here and below, the symbol \sim means equal up to $\mathcal{O}(\Gamma^2)$, and we will replace γ by the physically more meaningful transition rate Γ . As we will see below, Eq. (8) is valid as long as $\Gamma t \ll 1$.

Analyzing this result for different functional forms for $f_\lambda(t)$, we find that the coupling to the far environment is indeed slowing down the decoherence in the central system. However, the effect can be more or less pronounced. For generic systems, one often finds that $f_\lambda(t)$ changes from an exponential decay in the Fermi golden rule regime to a Gaussian decay in the perturbative regime [16, 22].

In the Fermi golden rule regime the effect is zero, which can also be understood in physical terms. In that regime the temporal correlations $\langle \tilde{V}_{\text{eff}}(t) \tilde{V}_{\text{eff}}(t') \rangle$ of the perturbation in the interaction picture decay very fast – on a time scale $t_{\text{corr}} \ll t_{\text{dec}}(\text{ce})$, the decoherence time in the central system. Therefore, even if the decoherence time in the near environment $t_{\text{dec}}(\text{ef})$ (due to the far environment) is smaller than $t_{\text{dec}}(\text{ce})$, as long as $t_{\text{dec}}(\text{ef}) > t_{\text{corr}}$, the far environment will not have any effect on the decoherence in the central system.

In the perturbative regime by contrast, $f_\lambda(t) = e^{-\lambda^2 t^2}$, such that $f_{\lambda,\Gamma}(t) \sim g_{\Gamma/\lambda}(\lambda t)$ with

$$g_\alpha(x) = (1 - \alpha x) e^{-x^2} + \alpha \sqrt{\pi/2} e^{-x^2/2} \text{erf}(x/\sqrt{2}). \quad (9)$$

For simplicity, we will compare our results to the exponentiated linear response (ELR) expression for the fidelity amplitude $f_\lambda(t)$ from Ref. [16], though note that an exact analytical result is also available [17, 18].

$$f_\lambda^{\text{ELR}}(t) = \exp[-\lambda^2 C(t)] \quad (10)$$

$$C(t) = t^2 + \pi t - 4\pi^2 \int_0^{t/(2\pi)} dt' \int_0^{t'} dt'' b_2(t''),$$

where $b_2(t)$ is the two-point form factor [23].

Caldeira-Leggett master equation: For full-fledged random matrix calculations, we would need to work in the Hilbert space of near and far environment. For the far environment, we would need a smaller mean level spacing in combination with a larger spectral span, as compared to the near environment. Still, in order to justify the use of RMT, we would need as many levels as possible also in the near environment. Such random matrix calculations are not viable, due to the dimension of the Hamiltonian matrices involved.

We will therefore use an approach which allows to work in the Hilbert space of the near environment alone, taking the effect of the far environment into account via a quantum master equation. For convenience we choose the Caldeira-Leggett master equation [19], where we replace the diagonal matrix representation of the harmonic oscillator Hamiltonian with a random matrix, defined as in Eq. (5). We choose both matrices H_0 and V_{eff} from the Gaussian orthogonal ensemble (GOE). We scale H_0 in such a way that the mean level spacing becomes one in the center of the spectrum. The matrix elements of V_{eff} are chosen to have the variances $\langle V_{ij}^{\text{eff}2} \rangle = 1 + \delta_{ij}$. In that way, the strength of the perturbation (implied by the dephasing coupling to the central system), measured in units of the mean level spacing, is given by λ . In the following figures we scale time by the Heisenberg time $t_H = 2\pi\hbar/d_0$. From earlier studies of similar models [7, 8], we know that the effect of the heat bath is quite compatible with the coupling to a further RMT environment in the Fermi golden rule regime, as long as the coupling to the heat bath, determined by Γ , is not

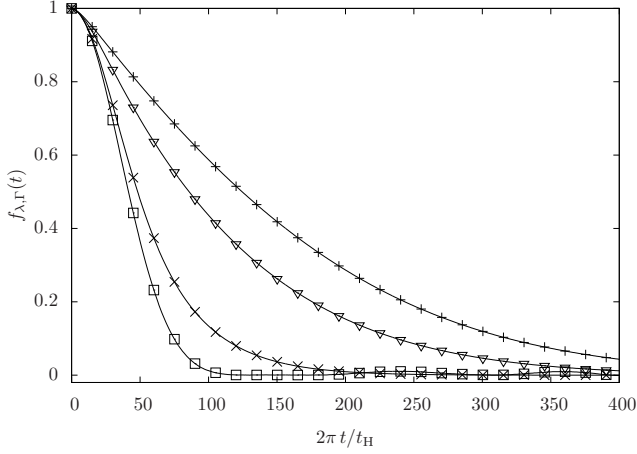


FIG. 1. Relative coherence $f_{\lambda,\Gamma}(t)$ in the Caldeira-Leggett model in the perturbative regime ($\lambda = 0.02$), for different values of the coupling to the heat bath alias far environment: $\Gamma/\lambda = 0$ (squares), 1.0 (shaped crosses), 5.0 (inverted triangles) and 10.0 (crosses). In all cases $N_e = 50$ and $n_{\text{run}} = 1000$ realizations.

too large. For the following simulations this conditions has been fulfilled.

Numerical simulations: The use of random matrices requires a Monte Carlo average over many realizations. Hence, choosing the dimension of the near environment to be $N_e = 50$, we perform numerical averages over $n_{\text{run}} = 1000$ realisations. The general behaviour of the relative coherence $f_{\lambda,\Gamma}(t)$ is shown in Fig. 1. For that figure, we choose $\lambda = 0.02$ for the dephasing perturbation (i.e. the perturbation due to the dephasing coupling), and different values for the coupling strength Γ between the near and far environment, as detailed in the figure caption. The figure clearly shows the announced effect, i.e. with increasing Γ , the coherence decays slower and slower.

The following three figures will allow us to evaluate the quality of our analytical result from Eq. (8). For a better quantitative comparison, we subtract the ELR approximation $f_{\lambda}^{\text{ELR}}(t)$ for pure fidelity decay, from both, the numerical simulation and the analytical approximation for $f_{\lambda,\Gamma}(t)$. Note that for the function $f_{\lambda}(t)$ appearing in the analytical expression, we use numerical results with much improved accuracy.[24]. The numerical result for $f_{\lambda,0}(t)$ differs from the ELR result due to the fact that $f_{\lambda}^{\text{ELR}}(t)$ is only an approximation, but also because of the varying level density over the spectral range of H_0 [25].

In Fig. 2 we consider the case $\lambda = 0.1$, where the dephasing perturbation is in the cross-over regime. Since we are plotting the difference $f_{\lambda,\Gamma}(t) - f_{\lambda}^{\text{ELR}}(t)$, the stabilizing effect of the far environment shows up as a growing positive hump. For each value of Γ , we plot three statistically independent numerical simulations. This gives us an idea about the statistical uncertainty of the results.

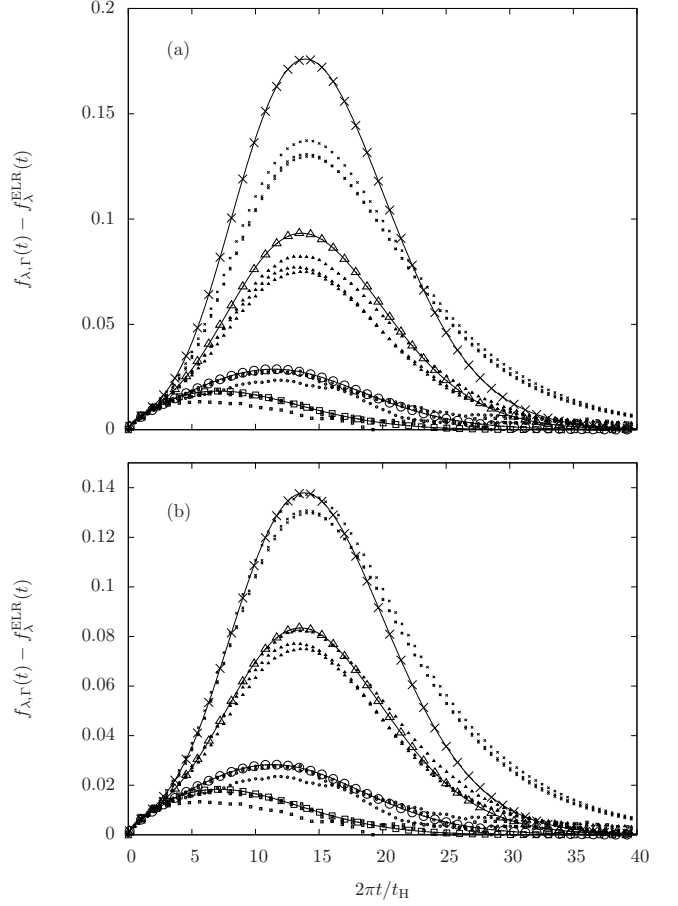


FIG. 2. (a) Coherence $f_{\lambda,\Gamma}(t)$ subtracted by the exponentiated linear response approximation $f_{\lambda}^{\text{ELR}}(t)$ to the fidelity amplitude, for $\lambda = 0.1$ (cross-over regime) and different values for the coupling to the heat bath: $\Gamma/\lambda = 0$ (squares), 0.1 (circles), 0.5 (triangles), and 1.0 (shaped crosses). The thick solid lines, show the analytical result according to Eq. (8), and the nearest thin dotted lines show three statistically independent ensemble averages for each case. (b) The same quantities as in panel (a), but for the theoretical curves we choose best fit values for the coupling to the heat bath: $\Gamma_{\text{fit}}/\lambda = 0.097$ (circles), 0.44 (triangles), and 0.77 (shaped crosses), obtained for the region $0 < t < 15$.

We can clearly see that the curves which correspond to $\Gamma = 0$ are different from zero, due to the reasons discussed above. Finally, we show three additional cases with increasing coupling to the heat bath. For those cases, the relative coupling strength $\alpha = \Gamma/\lambda$ is 0.1 (circles), 0.5 (triangles), and 1.0 (shaped crosses). We can observe that the theory agrees with the simulations, only in the case of smallest coupling, for stronger coupling the effect is systematically overestimated.

In Fig. 2(b) we intend to adjust the value for Γ (now denoted by Γ_{fit}) such that the theory agrees best with the numerical simulations. A good agreement between theory and simulations could not be achieved for all

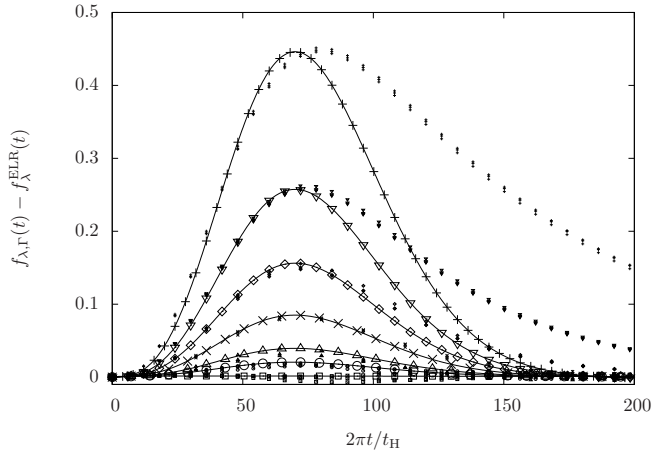


FIG. 3. Comparison between Caldeira-Leggett simulations and the linear response theory as in Fig. 2, but here for $\lambda = 0.02$ (perturbative dephasing perturbation). For the theoretical curves, we rescaled Γ_{fit} as explained in the text. The different cases shown are: (squares) $\Gamma = 0$, circles $\Gamma(\Gamma_{\text{fit}}) = 0.002(0.00195)$, triangles $0.004(0.0039)$, shaped crosses $0.01(0.00858)$, diamonds $0.02(0.0159)$, inverted triangles $0.04(0.0263)$, crosses $0.1(0.0457)$.

times, in particular not for moderate and strong coupling. However, a best fit for Γ_{fit} restricted to times up to the maximum which is always located at approximately $t_{\text{max}} \approx 15$, yields quite satisfactory results.

In Fig. 3 we repeat the comparison for $\lambda = 0.02$, where the coupling between central system and RMT environment is close to the perturbative regime. We use the same fitting procedure as in Fig. 2(b). However, in this case we consider a broader range of different values for $\alpha = \Gamma/\lambda$ which goes from $\alpha = 0.1$ until $\alpha = 10.0$. Essentially, we observe a similar behavior as in the case of $\lambda = 0.1$. However, it becomes also clear that a very large ratio Γ/λ yields stronger deviations between simulations and theory, even with fitted values for Γ and restricting ourselves to small times (here, $t \lesssim 60$). Nevertheless, the slowing down of decoherence in the central system due to the increasing coupling to the far environment, occurs just as before.

Finally, we compare in Fig. 4 the fitted values Γ_{fit} for the coupling to the far environment, with the nominal ones, by plotting $\Gamma_{\text{fit}}/\lambda$ versus Γ/λ . This is done for different dimensions of the near environment, for different coupling strengths between central system and near environment, and different couplings to the far environment. The derivation of our theoretical result within linear response theory showed that the deviation from the exact result should be quadratic in Γ . Hence, for sufficiently small values of Γ one would expect that the points in Fig. 4 would come close to the line $\Gamma_{\text{fit}} = \Gamma$. For larger values of Γ , we find that the effect of the far environment is smaller than predicted by our theory, as the fitted val-

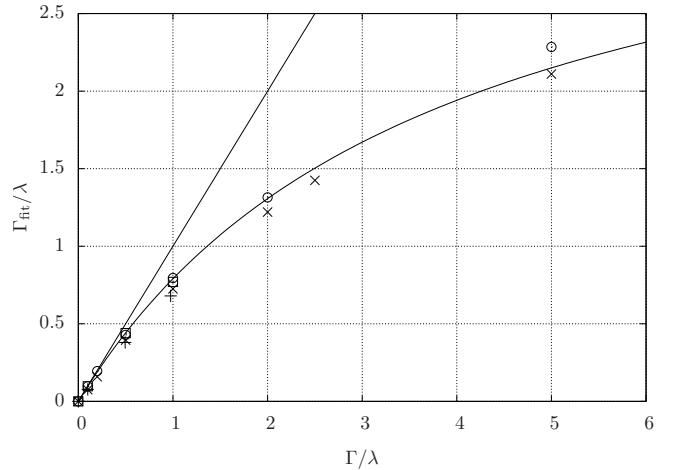


FIG. 4. $\Gamma_{\text{fit}}/\lambda$ vs. Γ/λ for $\lambda = 0.1$, $N_e = 25$ and $N_e = 50$ (crosses and squares respectively) and $\lambda = 0.02$, $N_e = 25$ (shaped crosses). The solid lines show the functions $\Gamma_{\text{fit}}/\lambda = \alpha$ and $b\alpha/(b+\alpha)$ with $b = 3.77$.

ues Γ_{fit} are smaller than the nominal ones. To guide the eye we plotted the straight line $\Gamma_{\text{fit}}/\lambda = \alpha$ as well as the function $g(\alpha) = b\alpha/(b+\alpha)$, with a best fit value $b = 3.77$, which describes the overall behavior of the points quite well.

Summarizing, we have been able to obtain an analytic expression confirming that nested environments can improve coherence of a central system as the coupling between near and far environment increases, as long as this coupling is small. We also extended previous limited numerical evidence for large coupling using a Caldeira-Leggett master equation which has been derived from RMT considerations in previous work [8]. This confirms that the effect subsists at large couplings between near and far environment, but subsides if the central system is strongly coupled to the near environment. An explanation using the quantum zeno effect is tempting but problematic due to the fact that we are considering weak couplings between near and far environment.

We thank P. Zanardi, L. Campos Venuti, C. Gonzalez, and C. Pineda for enlightening discussions, and we acknowledge the hospitality of the Centro Internacional de Ciencias, UNAM, where many of these discussions took place. We also acknowledge financial support from CONACyT through the grants CB-2009/129309 and 154586 as well as UNAM/DGAPA/PAPIIT IG 101113.

-
- [1] M. Brune, E. Hagley, J. Dreyer, X. Maître, A. Maali, C. Wunderlich, J. M. Raimond, and S. Haroche, *Phys. Rev. Lett.* **77**, 4887 (1996).
 - [2] J. M. Raimond, M. Brune, and S. Haroche, *Phys. Rev. Lett.* **79**, 1964 (1997).

- [3] H.-P. Breuer and F. Petruccione, *The Theory of Open Quantum Systems* (Oxford University Press, 2002).
- [4] J. Roden, W. T. Strunz, K. B. Whaley, and A. Eisfeld, *J. Chem. Phys.* **137**, 204110 (2012).
- [5] M. C. Nemes, (Private communication).
- [6] C. Pineda, C. González-Gutiérrez, and T. H. Seligman, (To be published (2015)).
- [7] J. Castillo, Master's thesis, Universidad de Guadalajara, 2011.
- [8] H. J. Moreno, Master's thesis, Universidad de Guadalajara, 2013.
- [9] C. González-Gutiérrez, Master's thesis, Universidad Nacional Autónoma de México, 2014.
- [10] P. Zanardi and L. Campos Venuti, *Phys. Rev. Lett.* **113**, 240406 (2014).
- [11] C. Pineda, T. Gorin, and T. H. Seligman, *New J. Phys.* **9**, 106 (2007).
- [12] T. Gorin, C. Pineda, H. Kohler, and T. H. Seligman, *New J. Phys.* **10**, 115016 (2008).
- [13] M. Carrera, T. Gorin, and T. H. Seligman, *Phys. Rev. A* **90**, 022107 (2014).
- [14] S. A. Gardiner, J. I. Cirac, and P. Zoller, *Phys. Rev. Lett.* **79**, 4790 (1997).
- [15] T. Gorin, T. Prosen, T. H. Seligman, and W. T. Strunz, *Phys. Rev. A* **70**, 042105:1 (2004).
- [16] T. Gorin, T. Prosen, and T. H. Seligman, *New J. Phys.* **6**, 20:1 (2004).
- [17] H.-J. Stöckmann and R. Schäfer, *New J. Phys.* **6**, 199:1 (2004).
- [18] H.-J. Stöckmann and R. Schäfer, *Phys. Rev. Lett.* **94**, 244101:1 (2005).
- [19] A. O. Caldeira and A. J. Leggett, *Physica* **121A**, 587 (1983).
- [20] E. Lutz and H. A. Weidenmüller, *Physica A* **267**, 354 (1999).
- [21] See Supplemental Material.
- [22] N. R. Cerruti and S. Tomsovic, *Phys. Rev. Lett.* **88**, 054103:1 (2002).
- [23] M. L. Mehta, *Random Matrices and the Statistical Theory of Energy Levels*, 3rd Edition (Academic Press, New York, 2004).
- [24] These are obtained from numerical simulations without far environment and some subsequent spline-fitting for facilitating the evaluation of the integral in Eq. (8). In that way, the accuracy can be greatly improved.
- [25] The remaining difference to the exact analytical expression found by Stöckmann and Schäfer [17, 18], is due to the fact that the trace in Eq. (7) includes the full spectral range where the level density varies according to the semi-circle law.

APPENDIX

Derivation of the main result (Eq. 8)

Dephasing coupling

Under dephasing coupling, the nondiagonal element of the qubit reduced state is just the fidelity amplitude of the RMT-environment with respect to the perturbation induced by the coupling between central system and near RMT environment. For an initial state Ω_0 , and with the abbreviation $H_\lambda = H_e + \nu_i V_e$,

$$\begin{aligned} f_\lambda(t) &= \text{tr} \left[\Omega_0 e^{i(H_0 + H_f + \gamma V_{e,f})t/\hbar} e^{-i(H_\lambda + H_f + \gamma V_{e,f})t/\hbar} \right] \\ &= \text{tr} \left\{ \left[e^{i(H_\lambda + H_f)t/\hbar} e^{-i(H_\lambda + H_f + \gamma V_{e,f})t/\hbar} \Omega_0 e^{i(H_0 + H_f + \gamma V_{e,f})t/\hbar} e^{-i(H_0 + H_f)t/\hbar} \right] e^{i(H_0 + H_f)t/\hbar} e^{-i(H_\lambda + H_f)t/\hbar} \right\}. \end{aligned} \quad (11)$$

The later two evolution operators are separable and therefore simplify as follows:

$$\begin{aligned} e^{i(H_0 + H_f)t/\hbar} e^{-i(H_\lambda + H_f)t/\hbar} &= e^{iH_0 t/\hbar} \otimes e^{iH_f t/\hbar} e^{-iH_\lambda t/\hbar} \otimes e^{-iH_f t/\hbar} \\ &= M_\lambda(t) \otimes \mathbb{1}_f, \quad M_\lambda(t) = e^{iH_0 t/\hbar} e^{-iH_\lambda t/\hbar}. \end{aligned}$$

Since $\text{tr}_f[A M \otimes \mathbb{1}_f] = A_{ij,kl} M_{km} \delta_{lj} = \text{tr}_f(A) M$ then

$$f_\lambda(t) = \text{tr}_e \left[\varrho_{e,f}(t) M_\lambda(t) \right], \quad \varrho_{e,f}(t) = \text{tr}_f \left[e^{i(H_\lambda + H_f)t/\hbar} e^{-i(H_\lambda + H_f + \gamma V_{e,f})t/\hbar} \Omega_0 e^{i(H_0 + H_f + \gamma V_{e,f})t/\hbar} e^{-i(H_0 + H_f)t/\hbar} \right]. \quad (12)$$

Linear response approximation for the coupling to the far environment

The trace over the far environment in Eq. (12) is almost exactly of the form as the reduced density matrix (in the interaction picture) treated in the reference [12], namely with $\mathcal{M}_\gamma(t) = e^{i(H_\lambda + H_f)t/\hbar} e^{-i(H_\lambda + H_f + \gamma V_{e,f})t/\hbar}$, we may write

$$f_\lambda(t) = \text{tr}_e \left[\tilde{\varrho}_e(t) M_\lambda(t) \right], \quad \tilde{\varrho}_e(t) = \text{tr}_f \left[\mathcal{M}_\gamma(t) \Omega_0 \mathcal{M}_\gamma(t)^\dagger \right]. \quad (13)$$

However, in order to apply the formalism of the reference [12], we should assume the coupling $V_{e,f}$ and the initial state Ω_0 to be separable:

$$\Omega_0 = \varrho_e \otimes \varrho_f, \quad V_{e,f} = v_e \otimes V_f, \quad \tilde{V}_{e,f}(t) = e^{i(H_\lambda + H_f)t/\hbar} v_e \otimes V_f e^{-i(H_\lambda + H_f)t/\hbar},$$

where we have already defined the representation $\tilde{V}_{e,f}(t)$ of the coupling operator to the far environment in the interaction picture. Of course there remains the very important difference, that here we have different echo operators on the left and the right side of the initial state. Nevertheless, following carefully the calculation made in [12], after the developed the echo operators into its Dyson series we find:

$$\begin{aligned} \varrho_{e,f}(t) &= \varrho_e - \frac{\gamma^2}{\hbar^2} (A_J - A_I), \quad A_J = \text{tr}_f [J(t) \Omega_0 + \Omega_0 J(t)^\dagger], \quad A_I = \text{tr}_f [I(t) \Omega_0 I(t)] \\ J_\lambda(t) &= \int_0^t d\tau \int_0^\tau d\tau' \tilde{V}_{e,f}(\tau) \tilde{V}_{e,f}(\tau'), \quad I_\lambda(t) = \int_0^t d\tau \tilde{V}_{e,f}(\tau). \end{aligned} \quad (14)$$

Now, note that $\tilde{V}_{e,f}(\tau)$ is separable, such that

$$\tilde{V}_{e,f}(\tau) = \tilde{v}_\lambda(\tau) \otimes \tilde{V}_f(\tau), \quad \tilde{v}_\lambda(\tau) = e^{iH_\lambda \tau/\hbar} v_e e^{-iH_\lambda \tau/\hbar},$$

and similarly for $\tilde{V}_f(\tau)$. The calculation for the average over $J_\pm(t)$ with respect to the random matrix V_f :

$$\langle J_\lambda(t) \rangle = \int_0^t d\tau \int_0^\tau d\tau' c(\tau - \tau') \tilde{v}_\lambda(\tau) \tilde{v}_\lambda(\tau') \otimes \mathbb{1}_f, \quad (15)$$

where $c(\tau)$ describes the spectral correlations of H_f and β is the Dyson parameter, such that for a GUE ($\beta = 2$) or a GOE ($\beta = 1$) with Heisenberg time $\tau_H = 2\pi\hbar/d_0$: $c(\tau) = 3 - \beta + \delta(\tau/\tau_H) - b_2(\tau/\tau_H)$. Similarly for A_I :

$$\langle A_I \rangle = \int \int_0^t d\tau d\tau' c(\tau - \tau') \tilde{v}_\lambda(\tau) \varrho_e \tilde{v}_\lambda(\tau'). \quad (16)$$

Finally, we obtain

$$\langle A_J - A_I \rangle = \int_0^t d\tau \int_0^\tau d\tau' c(\tau - \tau') \{ \tilde{v}_\lambda(\tau) [\tilde{v}_\lambda(\tau') \varrho_e - \varrho_e \tilde{v}_\lambda(\tau')] - [\tilde{v}_\lambda(\tau') \varrho_e - \varrho_e \tilde{v}_\lambda(\tau')] \tilde{v}_\lambda(\tau) \} \quad (17)$$

Fermi golden rule regime and master equation

If we assume that the Heisenberg time of the far environment τ_H is very large, and that we are in the Fermi golden rule regime for the coupling to the far environment, then from the correlation function $c(\tau)$, we only need to take the delta function into account. That reduces Eq. (17) to

$$\langle A_J - A_I \rangle = \frac{\tau_H}{2} \int_0^t d\tau [\tilde{v}_\lambda(\tau) \tilde{v}_\lambda(\tau) \varrho_e - 2 \tilde{v}_\lambda(\tau) \varrho_e \tilde{v}_\lambda(\tau) + \varrho_e \tilde{v}_\lambda(\tau) \tilde{v}_\lambda(\tau)] \quad (18)$$

Next, we will average that expression over the coupling matrix v_e , which is the near environment part of the coupling between near and far environment. Since this matrix is assumed to be an element of the GUE, we find:

$$\langle v_e^2 \rangle_{ik} = \sum_j v_{ij} v_{jk} = N_e \delta_{ik} \quad \Rightarrow \quad \langle v_e^2 \rangle = \langle \tilde{v}_\lambda(\tau) \tilde{v}_\lambda(\tau) \rangle = N_e \mathbb{1}_e \quad (19)$$

On the other hand, we find

$$\begin{aligned} \langle \tilde{v}_\lambda(\tau) \varrho_e \tilde{v}_\lambda(\tau) \rangle_{iq} &= (u^\dagger)_{ij} (v_e)_{jk} (u)_{kl} \varrho_{lm}^e (u^\dagger)_{mn} (v_e)_{np} (u)_{pq} \\ &= (u^\dagger)_{ij} \delta_{kn} \delta_{jp} (u)_{kl} \varrho_{lm}^e (u^\dagger)_{mn} (u)_{pq} = (u^\dagger)_{ij} (u)_{kl} \varrho_{lm}^e (u^\dagger)_{mk} (u)_{jq} \end{aligned} \quad (20)$$

This can be written as

$$\langle \tilde{v}_\lambda(\tau) \varrho_e \tilde{v}_\lambda(\tau) \rangle_{iq} = [M(\tau)^\dagger]_{iq} \text{tr}[\varrho_e M(\tau)] \quad \text{since} \quad M(\tau) = u^\dagger u, \quad M(\tau)^\dagger = u^\dagger u. \quad (21)$$

Therefore, we obtain for $\varrho_{e,f}(t)$:

$$\varrho_{e,f}(t) = \varrho_e - \frac{\gamma^2 \tau_H}{2\hbar^2} \left(2 N_e t \varrho_e - 2 \int_0^t d\tau \operatorname{tr}[\varrho_e M(\tau)] M(\tau)^\dagger \right) \quad (22)$$

Let us denote $\Gamma = \gamma^2 \tau_H N_e / \hbar^2$. Then we obtain for the fidelity amplitude:

$$f_{\lambda,\Gamma}(t) = \operatorname{tr} \left[(1 - \Gamma t) \varrho_e M(t) + \frac{\Gamma}{N_e} \int_0^t d\tau \operatorname{tr}[\varrho_e M(\tau)] M(\tau)^\dagger M(t) \right] \quad (23)$$

thus

$$f_{\lambda,\Gamma}(t) \sim (1 - \Gamma t) f_\lambda(t) + \Gamma \int_0^t d\tau f_\lambda(\tau) f_\lambda(t - \tau) \quad (24)$$

where we have used that $f_\lambda(t) = \operatorname{tr}[\varrho_e M(t)]$ and $N_e f_\lambda(t - \tau) = \operatorname{tr}[M(t - \tau)]$. So $f_\lambda(t)$ denotes the fidelity amplitude in the near environment, if there is no coupling to the far environment ($\gamma = 0$). The first line is exact (in the limit $\Gamma t \ll 1$), assuming that no ensemble averaging has been applied with respect to H_e and V_e . The second line assumes self averaging for the quantities $\operatorname{tr}[\varrho_e M(\tau)]$ and $\operatorname{tr}[M(t - \tau)]$ which will probably hold for generic initial states ϱ_e and sufficiently large near environment ($N_e \gg 1$).
